Fish and Shellfish Immunology 87 (2019) 886–896

Contents lists available at ScienceDirect

Fish and Shellfish Immunology

journal homepage: www.elsevier.com/locate/fsi

Full length article

A novel CC chemokine ligand 2 like gene from ayu *Plecoglossus altivelis* is involved in the innate immune response against to *Vibrio anguillarum*

Li Yu[a,1], Chang-Hong Li[a,1], Jiong Chen[a,b,*]

[a] Laboratory of Biochemistry and Molecular Biology, School of Marine Sciences, Meishan Campus, Ningbo University, Ningbo, 315832, China
[b] Key Laboratory of Applied Marine Biotechnology of Ministry of Education, Meishan Campus, Ningbo University, Ningbo, 315832, China

ARTICLE INFO

Keywords:
CCL2L
Chemotaxis
Monocyte/macrophage activation
Plecoglossus altivelis
Survival rate
Vibrio anguillarum

ABSTRACT

Chemokine (C—C motif) ligand 2 (CCL2), also known as monocyte chemoattractant protein 1 (MCP-1), is one of the key chemokines that regulate migration and infiltration of monocytes/macrophages (MO/MΦ) in mammals. However, the functional repertoire of fish CCL2 remains unclear. Here, we identified a cDNA sequence encoding a novel CCL2-like protein (PaCCL2L) in ayu, *Plecoglossus altivelis*. Sequence analysis revealed that PaCCL2L grouped with CCL2 homologs, and is most closely related to Mexican tetra (*Astyanax mexicanus*) and zebrafish (*Danio rerio*) homologs. PaCCL2 transcripts were expressed in all tested tissues from healthy ayu, with the highest level in the spleen. Upon *Vibrio anguillarum* infection, PaCCL2L transcripts increased significantly in tested tissues, including the liver, spleen, and head kidney. We then produced the recombinant PaCCL2L mature peptide (rPaCCL2L) by prokaryotic expression and generated the corresponding antibodies (anti-PaCCL2L). A significant increase in PaCCL2L protein and mRNA expression was observed in ayu MO/MΦ following *V. anguillarum* challenge. Intraperitoneal injection of rPaCCL2L resulted in significantly improved survival and reduced tissue bacterial load in *V. anguillarum*-infected ayu. rPaCCL2L had a positive effect on the chemotaxis of MO/MΦ and neutrophils both *in vitro* and *in vivo*. Meanwhile, rPaCCL2L exhibited a positive effect on the chemotaxis of LPS-stimulated MO/MΦ (M1 type) *in vitro*, whereas it exhibited no chemotaxis effect on cAMP-stimulated MO/MΦ (M2 type). In addition, rPaCCL2L treatment exhibited an enhanced effect on MO/MΦ phagocytosis, bacterial killing, respiratory burst, and mRNA expression of proinflammatory cytokines, whereas anti-PaCCL2L treatment had an inhibitory effect. Our study demonstrates that PaCCL2L might play a role in the immune response of ayu against *V. anguillarum* infection through chemotactic recruitment and activation of MO/MΦ.

1. Introduction

Chemokines are a family of small cytokines best known for their role in controlling the migration of a wide variety of cell types, particularly leukocytes [1]. Chemokines are the largest family of cytokines, composed of approximately 50 endogenous chemokine ligands in humans and mice [2,3]. They have multiple roles in the organization of the immune system under basal conditions and during infection, and a crucial role of chemokines is the recruitment of different types of leukocytes from blood to the sites of inflammation [2,3]. Based on the number and location of conserved cysteine residues near the N-terminus of the protein, chemokines are classified into four subfamilies, designated CC, CXC, C, and CX3C (where X is any amino acid residue and C is cysteine) [2]. CC chemokines, distinguished by adjacent cysteine residues in a conserved position form the largest subfamily of ligands with at least 28 members in mammals and primarily attract mononuclear cell types [4]. Fish express more numbers of CC chemokines than those in mammals due to extensive lineage-specific, intrachromosomal tandem duplications [5]. For example, there are 81 and 64 putative CC chemokine genes in zebrafish (*Danio rerio*) [6] and channel catfish (*Ictalurus punctatus*) [7], respectively, suggesting that CC chemokines play particularly important roles in the fish immune system. However, only 8 CC chemokine genes were found in both tiger puffer (*Takifugu rubripes*) and spotted green pufferfish (*Tetraodon nigroviridis*), which is far less than that in the abovementioned species [6].

CC chemokine ligand 2 (CCL2), which is also known as monocyte chemoattractant protein-1 (MCP-1), is a member of the CC chemokine family. CCL2 is produced by a large variety of cell types such as

* Corresponding author. Laboratory of Biochemistry and Molecular Biology, School of Marine Sciences, Meishan Campus, Ningbo University, Ningbo, 315832, China.
E-mail addresses: chenjiong@nbu.edu.cn, jchen1975@163.com (J. Chen).
[1] These authors contributed equally to this work.

https://doi.org/10.1016/j.fsi.2019.02.019
Received 26 December 2018; Received in revised form 7 February 2019; Accepted 13 February 2019
Available online 21 February 2019

Table 1
Oligonucleotide primer sequences used for qRT-PCR.

Primer	Gene	Accession number	Nucleotide sequence (5′→3′)	Amplicon size (bp)
PaCCL2LF	CCL2L	MG869684	CATGAGATGCTGTACAGACT	108
PaCCL2LR			ACA GCCGGCATGTTGCAGA	
PaTNFαF	TNF-α	JP740414	ACATGGGAGCTGTGTTCCTC	115
PaTNFαR			GCAAACACACCGAAAAAGGT	
PaIL-1βF	IL-1β	HF543937	TACCGGTTGGTACATCAGCA	104
PaIL-1βR			TGACGGTAAAGTTGGTGCAA	
PaIL-10F	IL-10	JP758157	TGCTGGTGGTGCTGTTTATGTGT	73
PaIL-10R			AAGGAGCAGCAGCGGTCAGAA	
PaTGFβF	TGF-β	JP742920	CTGGAATGCCGAGAACAAAT	101
PaTGFβR			GATCCAGAACCTGAGGGACA	
PaIL-6F	IL-6	MG264003	ACCTCACATTTCGCCTTCATACTAA	273
PaIL-6R			TGGCGTGGACAGTGTGTAGTATTTA	
PaIFN-γF	IFN-γ	JP730075	GCAACATAAACTTCAGGCGAATAAA	258
PaIFN-γR			CGAGGGAAGTAGTGTTTCTGGATTT	
Pa18SF	18S rRNA	FN646593	GAATGTCTGCCCTATCAACT	116
Pa18SR			GATGTGGTAGCCGTTTCT	

epithelial cells, fibroblasts, astrocytes, monocytes, and microglial cells, and mainly recruits monocytes, T-cells, and dendritic cells to the sites of inflammation [8,9]. CCL2 expression is increased in mouse models of bacterial infection or cecal ligation and puncture (CLP)-induced sepsis, and its upregulation causes the recruitment of leukocytes (mainly monocytes or macrophages) to sites of infection, which improves bacterial clearance and the survival rate [10–12]. Recruitment of macrophages and dendritic cells to the sites of infection was inhibited in CCL2 knockout (KO) mice or in mice administered with anti-CCL2 antibodies, causing a decrease in bacterial clearance and the survival rate [11,12]. The functions of CCL2 are known to be mediated by binding to the CCR2 receptor, a member of the G protein-coupled receptor family [9]. Recently, some nucleotide sequences similar to CCL2 (designated as MCP-1b-like, CCL2, and CCL2L) from fish such as zebrafish, Nile tilapia (*Oreochromis niloticus*), common carp (*Cyprinus carpio*), goldfish (*Carassius auratus*), Japanese ricefish (*Oryzias latipes*), tiger puffer, and large yellow croaker (*Larimichthys crocea*) have been identified and deposited in the GenBank database. However, these fish sequences share quite low sequence identities with mammalian CCL2, and their functions remain unclear.

Ayu (*Plecoglossus altivelis*), the member of the order Osmeriformes family Plecoglossidae, is an important economically cultured fish species in Japan, China, and Korea. However, rapid development of the ayu industry in China has been severely threatened by *Vibrio anguillarum* infection that results in both production and animal welfare problems [13]. Considering the vital roles of chemokines in the inflammatory response [14], it is worthwhile to study the biological functions of fish chemokines involved in disease. In the present study, we characterized a novel CCL2L gene from ayu (PaCCL2L). We analyzed the tissue mRNA expression of PaCCL2L in ayu upon *V. anguillarum* infection. We overexpressed the recombinant PaCCL2L (rPaCCL2L) in *Escherichia coli* and prepared the corresponding antibodies (anti-PaCCL2L). The chemotactic activity of PaCCL2L to neutrophils and to resting and polarized monocytes/macrophages (MO/MΦ) was investigated. Additionally, the immunomodulatory effect of PaCCL2L *in vivo* and its effect on MO/MΦ activation *in vitro* were also determined.

2. Materials and methods

2.1. Fish maintenance

Healthy ayu weighing 40–50 g each without any pathological signs were obtained from a commercial farm in Ninghai County, Ningbo City, China. Fish were kept in freshwater tanks in a recirculating system at 20–22 °C for 2 weeks of acclimation prior to the start of the experiments. All experiments were performed according to the Experimental Animal Management Law of China and were approved by the Animal Ethics Committee of Ningbo University.

2.2. Sequence characterization of PaCCL2L

The cDNA sequence of PaCCL2L was identified from a previously sequenced ayu head kidney-derived MO/MΦ transcriptome [15], and was authenticated by further cloning, sequencing, and comparison with similar sequences using a BLAST search (http://blast.ncbi.nlm.nih.gov/Blast.cgi). The Latin name and accession numbers of PaCCL2L and the related sequences used for analyses are provided in Supplementary file 1. Multiple alignments were analyzed using the ClustalW program (http://clustalw.ddbj.nig.ac.jp/) and a phylogenetic tree was constructed using MEGA version 6.0 [16]. The cleavage site of the signal peptide was predicted using the SignalP 4.1 program (http://www.cbs.dtu.dk/services/SignalP/). The protein domain architecture was predicted using the SMART program (http://smart.emblheidelberg.de/).

2.3. In vivo bacterial challenge and mRNA expression analysis of PaCCL2L

In vivo bacterial challenge was carried out as reported previously [17]. Briefly, *V. anguillarum* isolate ayu-H080701 was grown in nutrient broth at 28 °C, and collected when it was in the logarithmic growth phase. Ayu were infected by intraperitoneal (i.p.) injection of 1.2×10^4 colony-forming units (CFU) of *V. anguillarum* (in 100 μl PBS) per fish for the infected group, whereas the same volume of PBS was used for the control group. The liver, head kidney, and spleen were collected for total RNA extraction at 4, 8, 12, and 24 h post infection (hpi), after which they were immediately snap-frozen in liquid nitrogen. The RNA of healthy fish tissues, including the muscle, brain, gill, skin, heart, spleen, trunk kidney, head kidney, liver, and intestine, were also extracted for tissue expression pattern analysis.

Total RNA extraction, DNase I digestion, first-strand cDNA synthesis, and real-time quantitative PCR (qRT-PCR) were conducted as reported previously [18]. qRT-PCR was used to determine the mRNA expression of PaCCL2L in selected ayu tissues. The primers used are listed in Table 1. qRT-PCR was performed on an ABI StepOne Real-Time PCR System (Applied Biosystems, Foster City, USA), using SYBR premix Ex Taq II (TaKaRa, Dalian, China), as follows: (1) 40 cycles of amplification at 95 °C for 30 s and 60 °C for 20 s; (2) melting curve analysis at 95 °C for 5 s, 65 °C for 15 s, and 95 °C for 15 s, and (3) cooling at 40 °C for 30 s. Relative gene expression of PaCCL2L in healthy ayu was calculated using the $2^{-\Delta CT}$ method, with PaCCL2L normalized against Pa18S rRNA (the internal control). Relative gene expression of PaCCL2L in *V. anguillarum*-infected ayu was also normalized to that of Pa18S rRNA using the $2^{-\Delta\Delta CT}$ method. The experiment was repeated four times, and each qRT-PCR was performed in triplicate.

2.4. Prokaryotic expression and antibody preparation

The primers PaCCL2LpF: 5′-CGAATTCAGTGTCATGAGATGCTG TAC-3′, and PaCCL2LpR: 5′—CCTCGAGTCAGTTTTTAGCTTTTTTGG ACG-3′ were designed to amplify the PaCCL2L sequence encoding the mature peptide. Following digestion with *EcoR* I and *Xho* I (TaKaRa), the amplicon was cloned into the pET-32a (+) expression vector, and the constructed plasmid was subsequently transformed into *E. coli* BL21 (DE3). The expression of recombinant PaCCL2L protein with a TrxA-His-tag (rPaCCL2L) was induced by isopropyl-β-D-thiogalactopyranoside (IPTG), and the protein was purified using a nickel-nitrilotriacetic acid (Ni-NTA) column (TaKaRa). The purity of rPaCCL2L was determined by SDS-polyacrylamide gel electrophoresis (SDS-PAGE). The possibility of contamination of the rPaCCL2L preparation with endotoxins was investigated using the *Limulus amebocyte* lysate test as described previously [17]. Endotoxin in the recombinant proteins was less than 0.1 EU/mg after toxin removal with an endotoxin-removal column (Pierce, Rockford, IL). Then, purified rPaCCL2L was used as an antigen to produce antiserum by rabbit immunization. The anti-rPaCCL2L IgG (anti-PaCCL2L) and rabbit isotype IgG were purified from serum using Protein A agarose beads (Invitrogen, Shanghai, China), and their concentrations were measured using the Bradford method. The specificity of the antibody was tested by western blotting and visualized using an enhanced chemiluminescence (ECL) kit (Advansta, Menlo Park, USA), as described in section 2.7.

2.5. Primary culture of ayu MO/MΦ

The head kidney-derived MO/MΦ was isolated from healthy ayu as described previously [19]. Isolated MO/MΦ were seeded into 35 mm dishes (2×10^7/mL) and cultured in complete medium (RPMI 1640, 5% FBS, 5% ayu serum, 100 U/ml penicillin, and 100 μg/ml streptomycin) at 24 °C in 5% CO_2 after washing off the non-adherent cells.

2.6. Isolation of blood neutrophils

Cells were isolated from the caudal vein blood of healthy ayu according to a previously described method [17]. Briefly, heparinized blood was collected, and cells were isolated following sedimentation with 6% dextran T 500 (Sigma, St. Louis, USA). After centrifugation at 400 × *g* for 25 min, cells packed below Ficoll-Hypaque PREMIUM (*i.e.*, erythrocytes and neutrophils) were subjected to hypotonic lysis with ice-cold ACK (Ammonium-Chloride-Potassium) Lysis Buffer (0.15 M NH_4Cl, 0.01 M $KHCO_3$, 0.1 mM EDTA) to eliminate the red blood cells. The resulting neutrophil suspension was washed and suspended in RPMI 1640 medium. The purity of the ayu neutrophils isolated was greater than 95% as measured by Wright-Giemsa staining.

2.7. Changes of PaCCL2L mRNA/protein expression in ayu MO/MΦ upon bacterial challenge

Stimulation of MO/MΦ with *V. anguillarum* was performed as described previously [20]. Before infection, the medium was changed to antibiotic-free medium and cells were incubated for another 12 h. MO/MΦ were infected with live *V. anguillarum* at a multiplicity of infection (MOI) of 2. The control group was treated with PBS. Bacterial infected or PBS-treated cells were harvested at 0, 4, 8, 12, and 24 hpi, respectively. Total RNA was extracted from cells using RNAiso reagent (TaKaRa) and the mRNA expression of PaCCL2L in MO/MΦ was examined by qRT-PCR analysis as described in section 2.3. Simultaneously, cells were also lysed in buffer containing protease inhibitors (20 mM Tris-HCl, 1 mM EDTA, 1% Triton X-100, 1 mM phenylmethanesulfonyl fluoride (PMSF), 10 mg ml^{-1} aprotinin, 10 mg ml^{-1} leupeptin, and 10 mg ml^{-1} pepstatin-A, pH 8.0), and total proteins were prepared. The protein concentration was measured using the Bradford method. Western blot analysis and enhanced chemiluminescence (ECL) detection were performed as described previously [18]. The protein level of PaCCL2L was determined using the NIH ImageJ software and was normalized to a "housekeeping protein" glyceraldehyde-3-phosphate dehydrogenase (PaGAPDH) (anti-GAPDH monoclonal antibody from mouse; Beyotime Institute of Biotechnology, Shanghai, China). Three biological replicates were used for each treatment.

2.8. Fish survival and bacterial load assay

Ayu were divided into four groups of 16 fish each for the survival assays. Fish were injected intraperitoneally (i.p.) with 1.2×10^4 CFU/fish live *V. anguillarum* and then injected with 0, 1.0, 10.0, or 100.0 ng/g rPaCCL2L at 30 min after bacterial infection. Morbidity was monitored for 7 days after challenge, and mortality was recorded every 24 h. The Kaplan-Meier method was used to assess the survival rate.

RNA extracted from a *V. anguillarum* culture at a concentration of 1.0×10^9 CFU/ml was serially diluted 10-fold in sterile PBS, and each sample was determined by qRT-PCR using primers p2F and p2R to construct a standard curve for the calculation of bacterial numbers [21,22]. For the bacterial load assay, ayu were divided into three groups of 6 fish each. Each fish was injected i.p. with 1.2×10^4 CFU of *V. anguillarum* and with 0, 1.0, or 10.0 ng/g rPaCCL2L at 30 min after bacterial infection. Then the liver, spleen, and head kidney were collected at 24 hpi for qRT-PCR using the primers p2F: 5′—CCTTTAACC AAGTGGGCGTA-3′ and p2R: 5′-CGATTTGTAAGGGCGACAAT-3′) for the *V. anguillarum* metalloprotease (MP) gene [22]. The Ct values obtained from qRT-PCR were used to calculate the total number of CFU/ml present in all samples, based on the previously generated standard curve.

2.9. In vitro chemotaxis assay

In vitro cell chemotaxis assays were performed in a 24-well transwell chamber (Corning, NY, USA). rPaCCL2L (1.0 or 10.0 ng/ml) or heat inactivated (Hi) rPaCCL2L (10.0 ng/ml) in complete medium was added to the lower chambers, and 2×10^6 cells of ayu MO/MΦ or neutrophils were plated in the upper chambers. The chambers were incubated for 4 h at 24 °C. Cells that migrated from the upper to the lower chambers were counted using light microscopy (Nikon, Tokyo, Japan). Each migration assay was performed in quadruplicate.

The migration of LPS- or cAMP-stimulated MO/MΦ toward rPaCCL2L was further determined. The isolated ayu head kidney MO/MΦ were treated with 10.0 μg/ml lipopolysaccharide (LPS) for 12 h or with 0.5 mg ml^{-1} cAMP for 6 h to prepare LPS-induced M1 type or cAMP-induced M2 type MO/MΦ, respectively [23]. The mRNA expression levels of M1/M2 polarization markers (TNF-α and IL-1β for M1, IL-10 and TGF-β for M2) was determined by qRT-PCR with Pa18S rRNA as the internal reference gene. The *in vitro* chamber assay was then used to determine the chemotactic effect of Hi rPaCCL2L or rPaCCL2L on M1 and M2 MO/MΦ, and the non-stimulated MO/MΦ were used as the control.

2.10. In vivo chemotaxis assay

The *in vivo* cell chemotaxis assay was conducted according to a previously described method [24]. Briefly, fish in experimental groups were i.p. injected with 10.0 ng/g rPaCCL2L or 10.0 ng/g Hi rPaCCL2L, whereas fish in the control group received equal volumes of PBS. The peritoneal cells were collected at 24 h after treatment by rinsing with a sterilized syringe containing 2 ml PBS. After centrifugation at 2000 rpm for 8 min, cell pellets were obtained and resuspended in 1 ml of PBS. Direct counts of cells were performed using a hemocytometer. MO/MΦ and neutrophils were further identified microscopically by Wright-Giemsa staining.

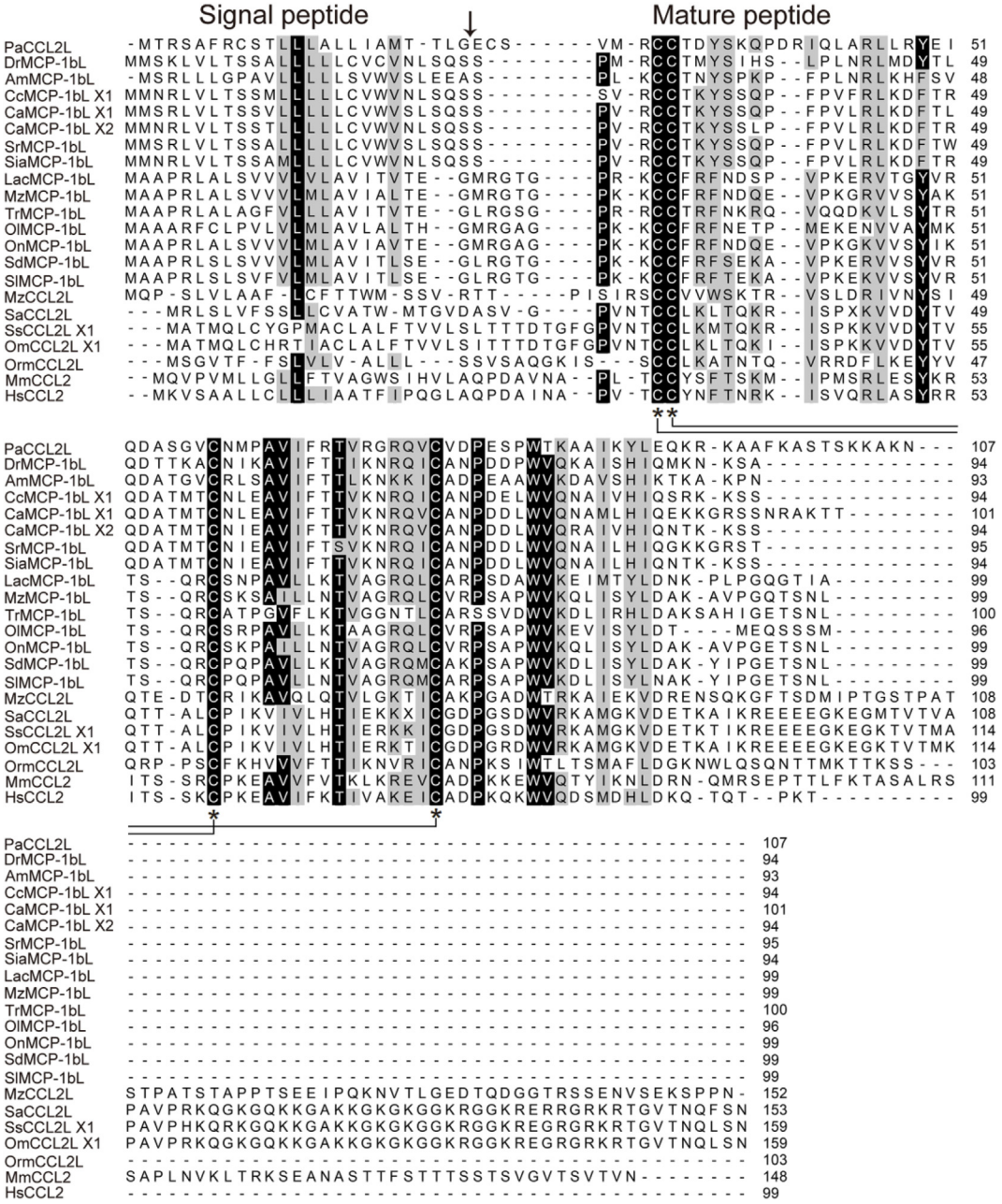

Fig. 1. Multiple alignment of PaCCL2L amino acid sequences and related sequences. Threshold for shading was 70%; similar residues are marked with a gray shadow, identical residues with a black shadow, and alignment gaps with "-". Predicted cleavage site for the signal peptide or mature peptide is marked as "↓". Conserved four cysteine residues are marked as "*". Two cysteine residues joined by a solid line represent a disulfide bond. Abbreviations of gene names are listed in Supplementary file 2.

2.11. Respiratory burst assay

The respiratory burst assay for ayu MO/MΦ was determined by measuring the concentration of intracellular O_2^- using the Nitro Blue Tetrazolium (NBT) reduction test as described previously [25]. Briefly, ayu MO/MΦ were pretreated with 10.0 ng/ml rPaCCL2L for 12 h or 250 μg/ml anti-PaCCL2L or rabbit isotype IgG for 30 min. The cells were then infected with live *V. anguillarum* at an MOI of 10. NBT was added to each plate at a final concentration of 1.0 mg ml^{-1} and the cells were incubated for 1 h at 24 °C. The reaction was stopped by adding 400 μl of 70% methanol, and the cells were then washed and air-dried. Formazan was dissolved in 120 μl of 2 M KOH and 140 μl of dimethyl sulfoxide (DMSO). The optical density at 620 nm (OD_{620}) was measured using an Ultrospec 1100 Pro UV/visible spectrophotometer (Amersham Biosciences, Piscataway, USA).

2.12. Effect of PaCCL2L on cytokine gene expression in MO/MΦ

To identify the role of PaCCL2L in the immune functions of ayu MO/MΦ, we evaluated its effect on cytokine expression during *V. anguillarum* infection. The isolated ayu head kidney MO/MΦ were seeded in a plate and then pretreated with 10.0 ng/ml rPaCCL2L for 12 h or 250 μg/ml anti-PaCCL2L or rabbit isotype IgG for 30 min before infecting with live *V. anguillarum* for 12 h at an MOI of 10. The mRNA expression of inflammatory cytokines, including TNF-α, IL-1β, IL-6, and IFN-γ, in MO/MΦ was examined by qRT-PCR. The primers used here are listed in Table 1.

2.13. Effect of PaCCL2L on MO/MΦ phagocytosis

In vitro phagocytosis of ayu MO/MΦ was examined as described previously [23]. *E. coli* DH5α in the logarithmic growth phase were labeled with fluorescein isothiocyanate (FITC) (Sigma, Saint Louis, USA) and designated as FITC-DH5α. Ayu MO/MΦ were pretreated with 10.0 ng/ml rPaCCL2L for 12 h or with 250 μg/ml anti-PaCCL2L or rabbit isotype IgG for 30 min. The heat-killed FITC-DH5α were added to the medium at an MOI of 20 and incubated for another 30 min before thoroughly washing with sterile PBS to remove any extracellular particles. Trypan blue (0.4%) was used to quench the fluorescence outside the cell membrane. The MO/MΦ were harvested and resuspended in FACS buffer (PBS, 0.2% BSA, 0.1% sodium azide). The engulfed bacteria were examined using a Gallios flow cytometer (Beckman Coulter) and FlowJo software. Relative mean fluorescence intensity (MFI) of the anti-PaCCL2L- or rabbit isotype IgG-treated group was expressed as fold change relative to the value of the group not treated with bacteria, and the value of the isotype IgG-treated group was assigned a unit of 100. Three independent experiments were performed.

2.14. Effect of PaCCL2L on bacterial killing by MO/MΦ

After pre-incubation with 10.0 ng/ml rPaCCL2L for 12 h or with 250 μg/ml anti-PaCCL2L or rabbit isotype IgG for 30 min, ayu MO/MΦ were infected with live *V. anguillarum* at an MOI of 10. Bacterial uptake by MO/MΦ was allowed to occur for 30 min, at 24 °C in an atmosphere with 5% CO_2. Non-internalized *V. anguillarum* were removed by washing extensively with sterile PBS. One set of samples (the uptake group) was collected until RNA extraction. Another set of samples (the kill group) was further incubated for 1.5 h to allow bacterial killing before cell lysis. Cells were subjected to RNA template preparation and qRT-PCR analysis using the primers p2F and p2R. Bacterial survival was determined by dividing the number of CFU in the kill group by those in the uptake group. Three independent experiments were performed.

2.15. Statistical analysis

All the data are reported as mean ± SD. Statistical analysis of the results was conducted using one-way analysis of variance (ANOVA) using SPSS version 13.0 (SPSS Inc, Chicago, USA). *P* values less than 0.05 were considered statistically significant.

3. Results

3.1. Molecular identification and sequence analysis of PaCCL2L

The cDNA sequence of PaCCL2L was identified using a BLAST search and was submitted to GenBank database under accession number MG869684. The cDNA was 600 nucleotides (nt) in length and comprised a large open reading frame (ORF) of 324 nt, which was predicted to encode a 107 amino acids (aa) polypeptide with a calculated molecular weight (MW) of 12.05 kDa and an isoelectric point (*p*I) of 9.77. Multiple alignment showed that PaCCL2L contained a 23 aa signal peptide at its N-terminus, and four cysteine residues that formed the intra-domain disulfide bridges (Cys30–Cys58 and Cys31–Cys74), which is the characteristic structure of CC chemokines (Fig. 1). However, the sequences of fish CCL2L are variable in length and residues, especially at the C-terminus (Fig. 1). This phenomenon is also observed in mammalian CCL2, for example, mouse CCL2 has a much longer C-terminus than human CCL2 (Fig. 1).

Sequence comparisons revealed that the mature peptide of PaCCL2L shares no more than 38.0% aa identity with other fish CCl2 homologs, and shows the highest aa identity with the zebrafish homolog. Phylogenetic tree analysis based on mature peptide sequences showed that CCL2 homologs grouped together to form a cluster distinct from other known CCL19, CCL20, and CCL25 clusters (Fig. 2). PaCCL2L was most closely related with Mexican tetra (*Astyanax mexicanus*) and zebrafish homologs (Fig. 2).

3.2. Alteration of the PaCCL2L transcript in ayu upon V. anguillarum infection

qRT-PCR was performed to analyze the mRNA expression level of the PaCCL2L gene in different tissues of healthy and *V. anguillarum*-infected ayu. PaCCL2L transcripts could be detected in all tested tissues of healthy ayu, with the highest level detected in the spleen (Fig. 3A). When ayu were infected by *V. anguillarum*, PaCCL2L transcripts were significantly increased in the main immune tissues (the liver, spleen, and head kidney) at 4 hpi, compared to the control (Fig. 3B–D). In the liver, the mRNA expression level of PaCCL2L was upregulated by 20.34 fold at 4 hpi, and remained at similar levels until 24 hpi (Fig. 3B). In the head kidney, PaCCL2L transcripts were upregulated by 3.23 fold at 4 hpi, reached the highest (4.45 fold) at 8 hpi (Fig. 3C). In the spleen, PaCCL2L transcripts were upregulated by 38.17 fold at 4 hpi, then gradually decreased and returned to the control level at 24 hpi (Fig. 3D).

3.3. Prokaryotic expression of PaCCL2L and antibody preparation

SDS-PAGE analysis showed that the MW of rPaCCL2L was approximately 27.58 kDa, which was in accordance with that calculated from the sequence (9.58 kDa mature PaCCL2L plus 18.0 kDa TrxA-His-tag) (Supplementary Fig. S1). In addition, the antibody to the rPaCCL2L (anti-PaCCL2L) was also able to detect purified rPaCCL2L and native PaCCL2L in healthy ayu MO/MΦ, and the MW of native PaCCL2L in ayu MO/MΦ was also approximately 12 kDa, similar to that calculated from the sequence (Supplementary Fig. S1).

3.4. Alteration of PaCCL2L mRNA and protein expression in MO/MΦ upon V. anguillarum stimulation

PaCCL2L mRNA and protein expression levels in PBS− and *V. anguillarum*-stimulated ayu MO/MΦ were investigated by qRT-PCR and western blot analysis, respectively. Upon *V. anguillarum* stimulation, PaCCL2L mRNA expression increased significantly in MO/MΦ at all detected time points and reached a peak at 8 hpi (7.43 fold) (Fig. 4A), whereas PaCCL2L protein levels also increased and reached the peak at 24 hpi (4.74 fold) (Fig. 4B).

3.5. Effect of rPaCCL2L on the survival of V. anguillarum-infected ayu

To investigate whether the rPaCCL2L was effective against *V. anguillarum* infection, a survival rate assay was conducted. I.p. administration of various concentrations of rPaCCL2L had a significant influence on the 7-day survival rates. All fish without rPaCCL2L treatment died by day 7, whereas fish treated with 1.0, 10.0, or 100.0 ng/g rPaCCL2L achieved survival rates of 20%, 40%, and 10% on day 7, respectively (Fig. 5).

3.6. Effect of rPaCCL2L on the bacterial burden of V. anguillarum-infected ayu

To determine the effect of rPaCCL2L on bacterial proliferation and dissemination *in vivo*, the bacterial load was quantitated by qRT-PCR analysis in the liver, spleen, and head kidney following i.p. injection with different concentrations of rPaCCL2L in *V. anguillarum*-infected fish. rPaCCL2L-treated groups showed a significant reduction of *V. anguillarum* load in the liver, spleen, and head kidney at 24 h after *V. anguillarum* challenge compared to the saline-treated control group (Fig. 6). The higher the concentration of rPaCCL2L, the better was the efficiency (Fig. 6).

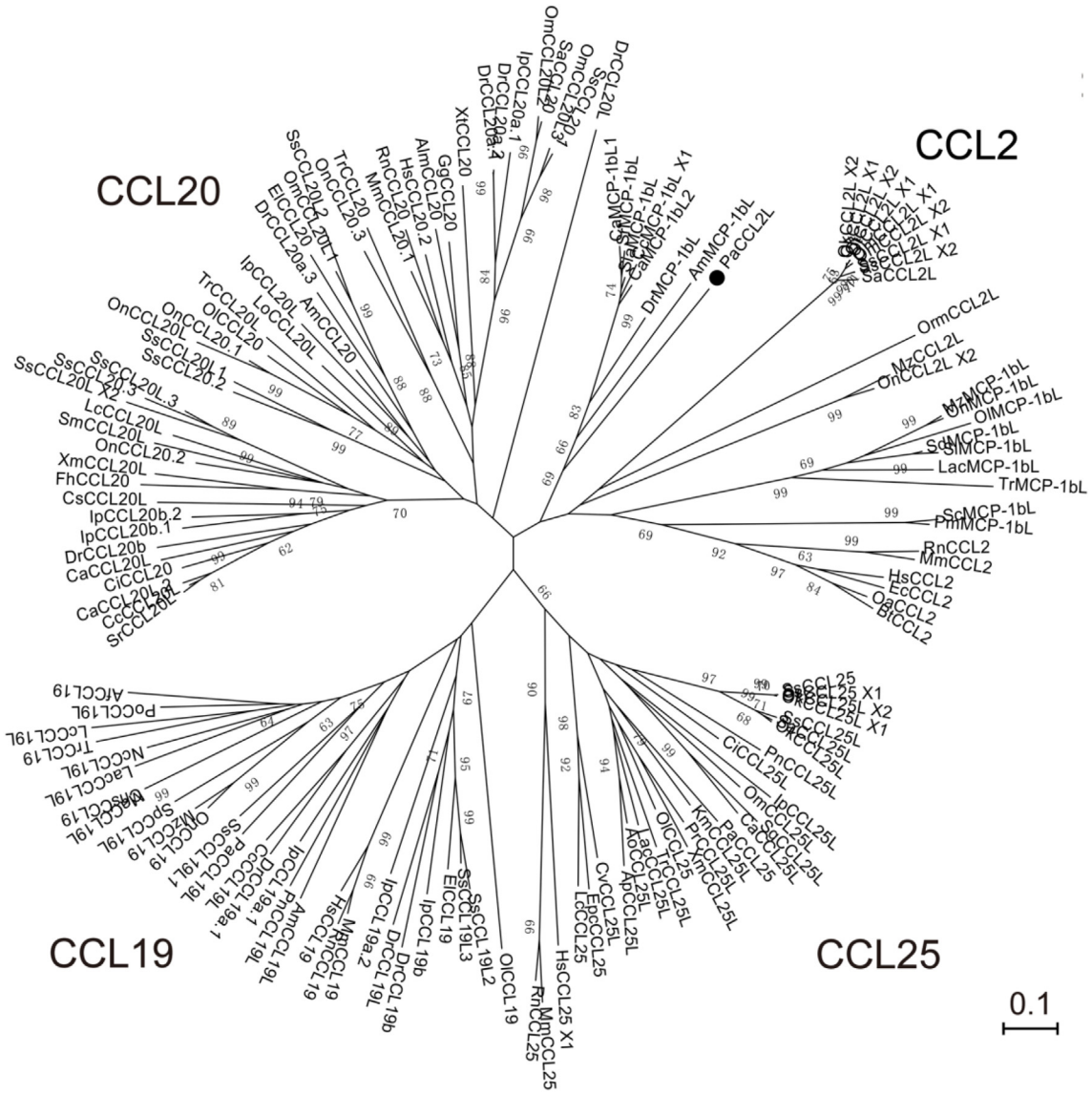

Fig. 2. Phylogenetic (neighbor-joining) analysis of the mature peptide sequence of PaCCL2L with other related sequences. The values at the forks indicate the percentage of trees in which this grouping occurred after bootstrapping (1000 replicates; shown only when > 60%). The scale bar indicates the number of substitutions per base. Abbreviations of gene names and accession numbers of sequences used are listed in Supplementary file 1.

3.7. Chemotactic activity of rPaCCL2L on resting MO/MΦ and neutrophils

In vitro transwell cell migration assay was conducted to test the chemotactic activity of rPaCCL2L. The results showed that 1.0 and 10.0 ng/ml rPaCCL2L both exhibited significant effect on the chemotaxis of resting MO/MΦ (Fig. 7A) and neutrophils (Fig. 7B) when compared with the control, whereas no significant difference was observed between the Hi rPaCCL2L-treated group and the control (Fig. 7A and B). The chemotactic activity of rPaCCL2L on resting MO/MΦ showed positive correlations associated with a dose-dependent effect (Fig. 7A), whereas that on neutrophils was dose-independent (Fig. 7B).

The numbers of migrated MO/MΦ and neutrophils in the abdominal cavity of ayu were also investigated at 24 h after i.p. administration of rPaCCL2L (Fig. 7C and D). rPaCCL2L administration induced an increase in MO/MΦ and neutrophil numbers in the abdominal cavity of ayu when compared with the control, but no significant difference was observed between the Hi rPaCCL2L-treated group and the control (Fig. 7C and D).

3.8. Chemotactic activity of rPaCCL2L on LPS- or cAMP-stimulated MO/MΦ

The mRNA expression levels of M1/M2 polarization markers was determined in LPS- or cAMP-stimulated ayu MO/MΦ. TNF-α and IL-1β were upregulated in LPS-stimulated MO/MΦ when compared with the control, whereas IL-10 and TGF-β showed no significant changes (Fig. 8A). However, IL-10 and TGF-β were upregulated in cAMP-stimulated MO/MΦ when compared with the control, whereas TNF-α and IL-1β showed no significant changes (Fig. 8A). This result suggested that LPS- and cAMP-stimulated MO/MΦ had M1 and M2 phenotypes, respectively.

The migration of LPS- or cAMP-stimulated MO/MΦ toward rPaCCL2L was determined. Relative to the control, rPaCCL2L induced LPS-stimulated MO/MΦ (M1 type) migration at a concentration of 1.0 ng/ml (18.4% cells) and 10.0 ng/ml (15.4% cells) (Fig. 8B and C). However, rPaCCL2L did not exhibit significant chemotactic activity in cAMP-stimulated MO/MΦ (M2 type) (Fig. 8B and C). In addition, 10.0 ng/ml Hi rPaCCL2L did not exhibit significant chemotactic activity in both M1 and M2 type MO/MΦ compared with the control (Fig. 8B

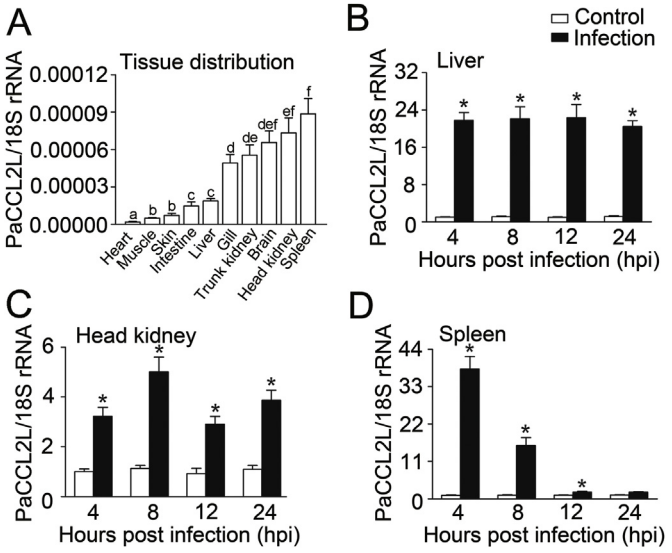

Fig. 3. qRT-PCR analysis of PaCCL2L expression patterns in healthy ayu tissues and immune tissues after *V. anguillarum* infection. (A) mRNA expression profiles of PaCCL2L in healthy ayu. Values denoted by different letters are significantly different when compared by ANOVA ($P < 0.05$). (B–D) PaCCL2L transcripts in immune tissues of ayu challenged with *V. anguillarum*. Tissues were collected at different time points post infection. The relative PaCCL2L transcript was normalized to Pa18S rRNA. The mRNA level in the 4 h PBS-injected group was normalized to 1. n = 4. *$P < 0.05$.

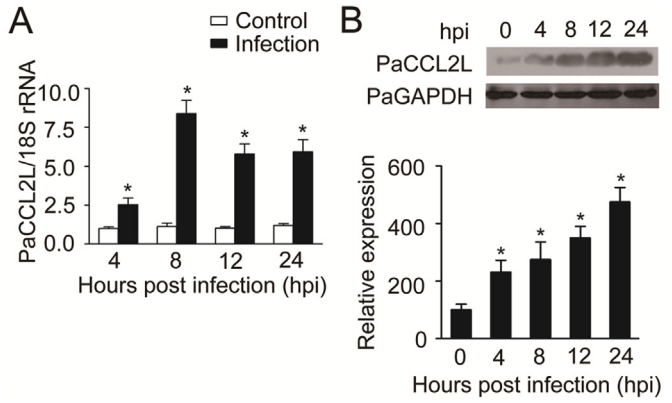

Fig. 4. Alteration of PaCCL2L mRNA and protein expression in ayu MO/MΦ upon *V. anguillarum* stimulation. (A) qRT-PCR was performed to analyze the mRNA expression of PaCCL2L in ayu MO/MΦ upon *V. anguillarum* stimulation. The cells in antibiotic-free medium were infected with live *V. anguillarum* at an MOI of 2. The control group was treated with an equal volume of PBS. The cells were collected at 4, 8, 12, and 24 hpi. PaCCL2L transcript levels were normalized to those of Pa18S rRNA, and the mRNA level in the 4 h PBS-treated group was normalized to 1. n = 5. *$P < 0.05$. (B) Western blot analysis of the changes in PaCCL2L protein levels in ayu MO/MΦ upon *V. anguillarum* stimulation at 0, 4, 8, 12, and 24 hpi. The histogram shows changes in the relative band intensity of PaCCL2L. The band intensity of PaGAPDH was set as the internal reference. The protein level at 0 hpi was normalized as 100. n = 3. *$P < 0.05$.

and C).

3.9. Effect of PaCCL2L on the respiratory burst of ayu MO/MΦ

Respiratory burst reflects the capacity of macrophages to use oxygen-dependent microbicidal mechanisms [26]. Therefore, we analyzed the alteration of respiratory burst in ayu MO/MΦ upon rPaCCL2L and anti-PaCCL2L treatment. rPaCCL2L enhanced the respiratory burst in ayu MO/MΦ. The absorbance values (OD_{620}) for the 10.0 ng/ml rPaCCL2L treated group were 1.72 ± 0.10, whereas those of the PBS treated group were 0.72 ± 0.16 (Fig. 9A). Anti-PaCCL2L inhibited the respiratory burst in ayu MO/MΦ. The OD_{620} value for the 250 μg/ml anti-PaCCL2L treated group was 0.52 ± 0.07, while that of the isotype IgG treated group was 0.75 ± 0.10 (Fig. 9B).

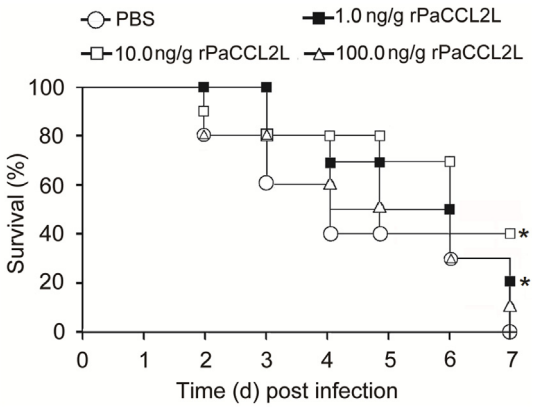

Fig. 5. Effect of treatment with rPaCCL2L at different concentrations on survival rate of ayu upon *V. anguillarum* infection. The fish in experimental groups received i.p. injection of 0, 1.0, 10.0, or 100.0 ng/g rPaCCL2L at 30 min after *V. anguillarum* infection, respectively. The control group received an equal volume of PBS. Fish were monitored for signs of sickness and mortality every 24 h for 7 days. n = 16. *$P < 0.05$.

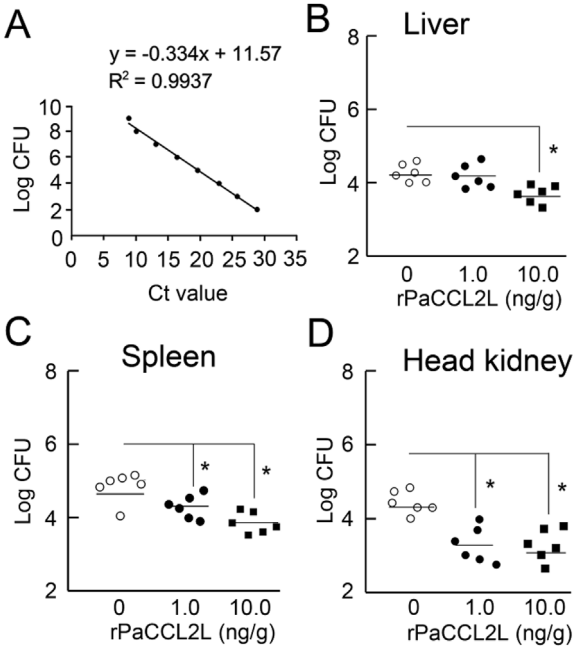

Fig. 6. The effect of rPaCCL2L treatment on bacterial load of *V. anguillarum*-infected ayu. Each fish was i.p. injected with live *V. anguillarum* at a dose of 1.2×10^4 CFU and 30 min later with an equal volume of 1.0 or 10.0 ng/g rPaCCL2L, respectively. The control group received an equal volume of saline. Fish were euthanized after 24 h and the liver, spleen, and head kidney were collected. (A) A standard curve was generated by qRT-PCR detection of 10-fold serial dilutions of *V. anguillarum*. (B–D) A qRT-PCR assay was used for the identification and quantification of *V. anguillarum* in ayu tissue. Colony numbers were normalized to 0.1 g tissue weight. Data represent the bacterial load in the liver, spleen, and head kidney. n = 6. *$P < 0.05$.

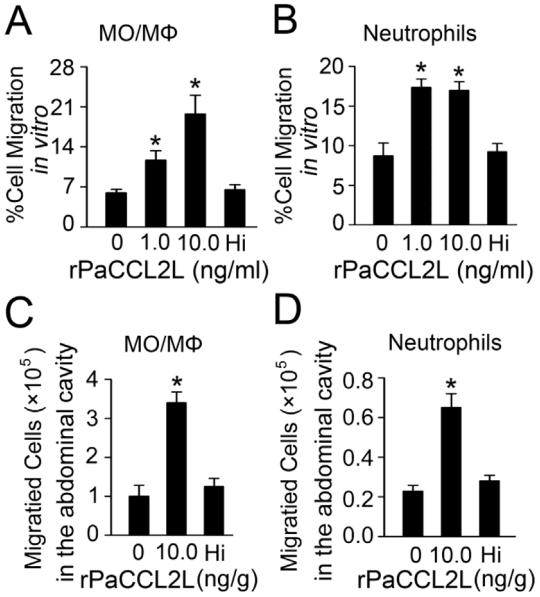

Fig. 7. Effect of rPaCCL2L on the chemotaxis of resting MO/MΦ and neutrophils. (A and B) *In vitro* analysis of the migration percentage of resting MO/MΦ and neutrophils toward rPaCCL2L at different concentrations (1.0 and 10.0 ng/ml, respectively) or 10.0 ng/ml Hi rPaCCL2L. The PBS-treated group (0 ng/ml rPaCCL2L) was used as the control. (C and D) *In vivo* analysis of the numbers of MO/MΦ and neutrophils in the abdominal cavity of ayu at 24 h after i.p. administration of 10.0 ng/g rPaCCL2L or 10.0 ng/g Hi rPaCCL2L, respectively. The PBS-treated group (0 ng/g rPaCCL2L) was used as the control. Cells were counted under a light microscope after Wright-Giemsa staining at 400 X magnification. Data are expressed as the mean ± SD and are representative of four independent experiments. $^{*}P < 0.05$.

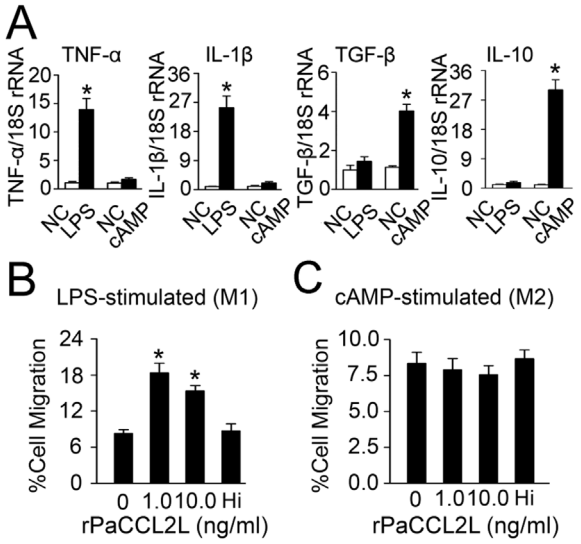

Fig. 8. Effect of rPaCCL2L on the migration of polarized ayu MO/MΦ. (A) The mRNA expression of M1/M2 polarization markers (IL-1β and TNF-α for M1 type; IL-10 and TGF-β for M2 type) in ayu MO/MΦ stimulated with LPS and cAMP. The transcript levels of cytokines were normalized to that of Pa18S rRNA, and the mRNA level in the non-stimulated group (control) was normalized to 1. (B and C) Effect of rPaCCL2L on the migration of LPS- or cAMP-stimulated MO/MΦ. The migration percentage of LPS- or cAMP-stimulated MO/MΦ was determined after incubation with rPaCCL2L or Hi rPaCCL2L for 4 h. Non-stimulated resting MO/MΦ were used as controls. Data are expressed as the mean ± SD of four independent experiments. $^{*}P < 0.05$.

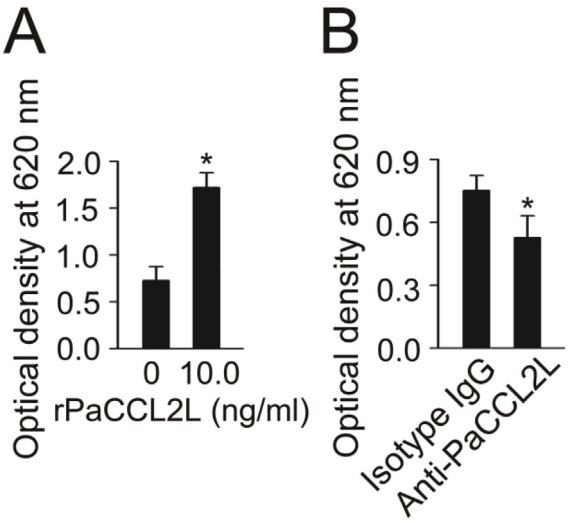

Fig. 9. Effect of PaCCL2L on the respiratory burst of ayu MO/MΦ. (A) Effect of rPaCCL2L on the respiratory burst of ayu MO/MΦ. Ayu MO/MΦ were pretreated with 10.0 ng/ml rPCCL2L for 12 h, and live *V. anguillarum* were then added at an MOI of 10. (B) Effect of anti-PaCCL2L on the respiratory burst of ayu MO/MΦ. MO/MΦ were pretreated with 250 μg/ml anti-PaCCL2L for 30 min, and live *V. anguillarum* were then added at an MOI of 10. NBT was added to each plate at a final concentration of 1 mg ml^{-1}. The respiratory burst of MO/MΦ was measured and expressed as OD_{620} value. Data are expressed as mean ± SD. n = 3. $^{*}P < 0.05$.

3.10. Effect of PaCCL2L on pro-inflammatory cytokine expression in MO/MΦ

Fish MO/MΦ are a major cellular source of important pro-inflammatory cytokines such as TNF-α, IL-1β, IL-6, and IFN-γ, and are necessary for the control of infection. Therefore, we investigated the effect of PaCCL2L on the mRNA expression of pro-inflammatory cytokines in ayu MO/MΦ upon *V. anguillarum* stimulation. qRT-PCR analysis revealed that the mRNA expressions of TNF-α, IL-1β, IL-6, and IFN-γ were significantly upregulated in ayu MO/MΦ treated with 10.0 ng/ml rPaCCL2L compared with the group without rPaCCL2L treatment (Fig. 10A–D). On the other hand, anti-PaCCL2L treatment significantly inhibited the mRNA expression of pro-inflammatory cytokines in ayu MO/MΦ compared with the isotype IgG-treated group (Fig. 10E–H).

3.11. Effect of PaCCL2L on the phagocytosis and bacterial killing of ayu MO/MΦ

As rPaCCL2L could alter cytokine mRNA expression and respiratory burst in MO/MΦ, we further analyzed its effect on phagocytosis and bacterial killing activity of MO/MΦ after bacterial infection. Phagocytosis of FITC-DH5α by rPaCCL2L pre-treated MO/MΦ was significantly higher (up to 1.85 fold) than that of the PBS treated group (Fig. 11A), whereas anti-PaCCL2L had an inhibitory effect on phagocytosis (down to 0.65 fold) (Fig. 11B).

In addition, qRT-PCR showed that the bacterial survival rate of the rPaCCL2L-treated group (38.74 ± 5.46%) was lower than that of the PBS group (65.89 ± 6.92%; Fig. 11C), whereas the bacterial survival rate of the anti-PaCCL2L-treated group (65.39 ± 6.46%) was higher than that of the control group (49.90 ± 5.14%; Fig. 11D).

4. Discussion

CCL2 is one of the key chemokines that regulate the migration and infiltration of MO/MΦ [27] and has been demonstrated to be induced and involved in various diseases. In fish, genes encoding CCL2

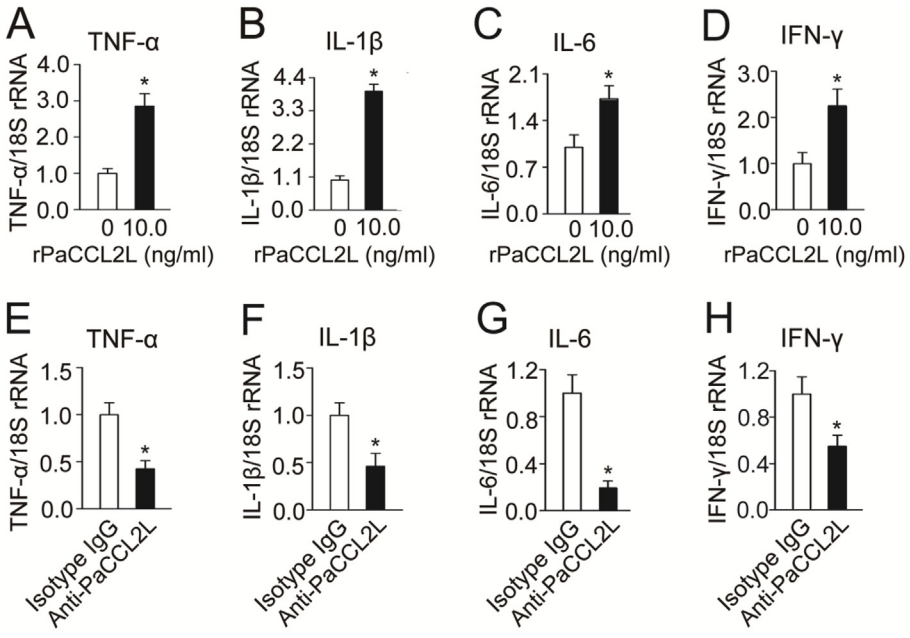

Fig. 10. Effect of PaCCL2L on the mRNA expression of pro-inflammatory cytokines in ayu MO/MΦ upon live *V. anguillarum* stimulation. (A-D) mRNA expression of TNF-α, IL-1β, IL-6, and IFN-γ in ayu MO/MΦ incubated with 0 or 10.0 ng/ml rPaCCL2L for 12 h before stimulation with live *V. anguillarum* for 12 h at an MOI of 10. (E-H) mRNA expression of TNF-α, IL-1β, IL-6, and IFN-γ in ayu MO/MΦ treated with anti-PaCCL2L (250 μg/ml) for 30 min before the stimulation with live *V. anguillarum* for 12 h at an MOI of 10. The mRNA transcript level of these four cytokines was determined by qRT-PCR and was normalized to the level of Pa18S rRNA. Data are expressed as mean ± SD. n = 3. $^*P < 0.05$.

homologs have been sequenced, but no study on their biological function has been published yet. In the present study, we identified a novel CCL2-like protein in ayu. PaCCL2L has the structural characteristics of CC chemokines and its mature peptide shares the highest aa identity of 38.0% with the zebrafish CCL2 homolog. Phylogenetic tree analysis revealed that PaCCL2L grouped with other known CCL2 homologs, and was most closely related to Mexican tetra and zebrafish homologs. Considering the structural conservation of CCL2-like proteins between fish and mammals, fish homologs might have similar functions as those reported in mammals.

In mammals, CCL2 expression levels can be induced by pathogen infection or endotoxin challenge. After 750 μg LPS administration, the protein levels of MCP-1 in the lung and liver of CD-1 mice increased rapidly and substantially up to 10 and 42 fold at 2 h, respectively, and the plasma MCP-1 level simultaneously increased from the undetectable level to 9.03 ± 1.9 ng/ml [28]. In the human monocytic cell line THP-1 and in primary monocytes, the mRNA and protein expression of CCL2 were both induced by infection with modified vaccinia virus Ankara (MVA) [8]. In human tumor stromal cells or cultured macrophages, *Helicobacter felis* strain ATCC 49179 infection or stimulation with LPS induced the mRNA expression of CCL2 [29]. In the present study, PaCCL2L was found to be constitutively expressed in the tested healthy fish tissues, with the highest level detected in the spleen. Upon *V. anguillarum* infection, PaCCL2L transcripts in the tested immune tissues or MO/MΦ were all significantly upregulated, which coincided with the results observed in mammalian CCL2 [8,28,29], suggesting that PaCCL2L is tightly involved in the immune response of fish against *V. anguillarum* infection.

Mammalian CCL2 is reported to contribute to the protective immunity against microbial infection or sepsis [10–12,30–32]. Treatment with recombinant CCL2 (rCCL2) increased the bacterial clearance and improved the survival rate of mice that were systemically infected with

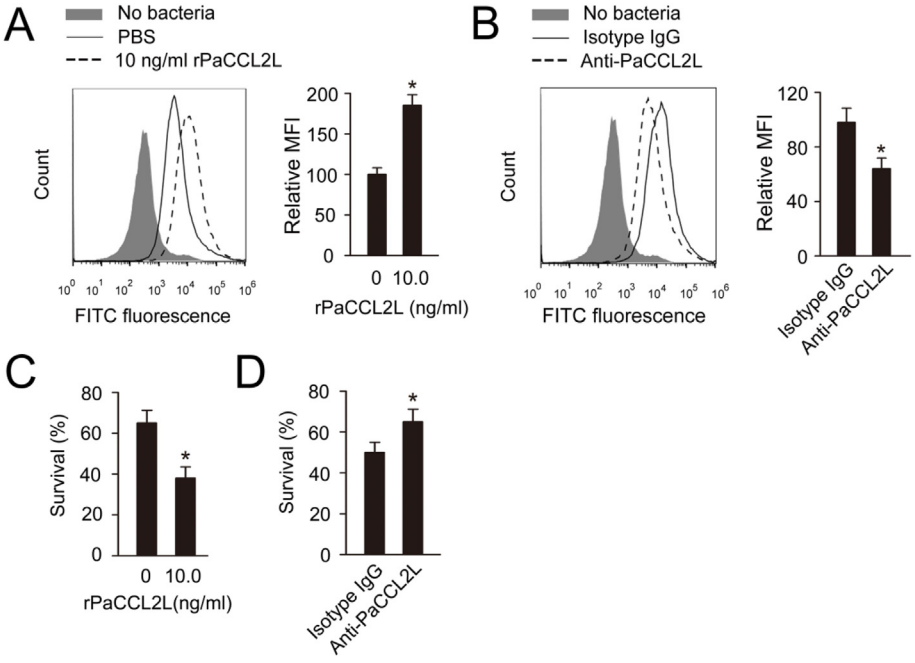

Fig. 11. Effect of PaCCL2L on the phagocytosis and bacterial killing of ayu MO/MΦ. (A, B) Effect of rPaCCL2L and anti-PaCCL2L on the phagocytosis of MO/MΦ. Ayu MO/MΦ were pre-treated with PBS or 10.0 ng/ml rPaCCL2L for 12 h, or with 250 μg/ml anti-PaCCL2L or isotype IgG for 30 min. FITC-DH5α was added at an MOI of 20 afterwards and incubated for an additional 30 min. Phagocytosis of FITC-DH5α was determined by flow cytometry analysis. MFI was presented as fold change over the control group (PBS-treated or isotype IgG-treated), which was assigned a unit of 100. n = 3. $^*P < 0.05$. (C, D) Effect of rPaCCL2L and anti-PaCCL2L on the bacterial killing of MO/MΦ. Ayu MO/MΦ were pre-treated with PBS or 10.0 ng/ml rPaCCL2L for 12 h, or with 250 μg/ml anti-PaCCL2L or isotype IgG for 30 min. Live *V. anguillarum* were added at an MOI of 10 and incubated for an additional 30 min. Killing of *V. anguillarum* by ayu MO/MΦ was measured using a CFU assay based on a standard curve. Data are expressed as mean ± SD. n = 3. $^*P < 0.05$.

Pseudomonas aeruginosa or *Salmonella typhimurium* [30]. CCL2 blockade with polyclonal anti-CCL2 antiserum significantly decreased the survival rate of septic mice and enhanced the number of bacterial CFUs from the peritoneum of CLP mice [32]. Pretreatment with anti-CCL2 monoclonal antibodies increased the number of bacterial CFUs recovered in the peritoneal lavage fluid of CLP mice [12]. In the present study, we found that administration of 10.0 ng/g rPaCCL2L to fish had the lowest mortality (60%) compared to that with 1.0 ng/g (80%) or 100.0 ng/g (90%) rPaCCL2 treatment. This effect was accompanied by a lowered bacterial burden. Our data is consistent with those reported for mammalian CCL2, confirming that PaCCL2L improved the outcome of ayu upon *V. anguillarum* infection.

CCL2 is known to play a crucial role in the recruitment of leukocytes to the site of infection. Recombinant human CCL2 induced the migration of human peripheral blood mononuclear cells (PBMC) and murine peritoneal macrophages in an *in vitro* chemotaxis assay [30,33]. Recombinant mouse CCL2 induced the migration of LPS-activated human polymorphonuclear leukocytes (PMNs) *in vitro* [34]. In mouse models of sepsis, recruitment of leukocytes such as macrophages, dendritic cells, and neutrophils depended on CCL2 [11,34]. Upon *S. pneumoniae* infection, the recruitment of lung exudate macrophages and conventional dendritic cells was impaired in CCL2 KO mice [11]. Neutrophil influx and macrophages were both reduced in the lungs of CCL2 KO mice after *E. coli* infection, and neutrophil influx was increased in bronchoalveolar fluid (BALF) when the CCL2 KO mouse received rCCL2 [34]. CCL2 overexpression in colon cancer cells or in rat gliosarcoma cells inhibits tumor development and is associated with recruitment of M1 macrophages at the site of injection [35,36]. In the present study, we determined the chemotactic activity of rPaCCL2L in ayu MO/MΦ and neutrophils *in vitro* and *in vivo*. We found that rPaCCL2L could attract neutrophils and MO/MΦ *in vitro* and *in vivo*, which is the same as that reported for mammalian CCL2 [11,30,33,34,37]. rPaCCL2L induced LPS-stimulated MO/MΦ (M1 type) migration, but did not exhibit significant chemotactic activity in cAMP-stimulated MO/MΦ (M2 type), which is coincident with previous reports [35,36]. Our results indicate that PaCCL2L is important for the migration of M1 type MO/MΦ and neutrophils in ayu.

Activation of MO/MΦ is a critical step in clearing bacteria [38]. Treatment of mouse peritoneal macrophages with anti-CCL2 antibodies after incubation with *E. coli* increased CFU numbers in the culture supernatant, whereas treatment of macrophages with recombinant CCL2 before incubation with *E. coli* decreased the CFU numbers [12]. Treatment with rCCL2 induced nitrite production in cultured peritoneal macrophages [12], and nitrite production was inhibited after LPS treatment in CCL2 KO mice [12]. Previous studies also revealed that CCL2 induced the expression of pro-inflammatory cytokines such as TNF-α and IL-6 [34,39]. TNF-α and IL-6 levels in the blood and BALF of CCL2 KO mice were significantly lower than those in wild type mice after *E. coli* infection, but MCP-1 KO mice reconstituted with rCCL2 (10 μg/mouse) showed an increased expression of TNF-α and IL-6 in BALF after *E. coli* infection [34]. Treatment with rCCL2 (100.0 ng/ml) upregulated the mRNA expression of TNF-α in RAW264.7 cells [39]. In the present study, we determined the effect of PaCCL2L on ayu MO/MΦ phagocytosis, intracellular bacterial killing, respiratory burst, and the expression of pro-inflammatory cytokines *in vitro*. We found that rPaCCL2L treatment increased the phagocytosis, intracellular bacterial killing and respiratory burst in ayu MO/MΦ, whereas anti-CCL2 treatment had an opposite effect. Moreover, rPaCCL2L upregulated the mRNA expression of selected pro-inflammatory cytokines, including TNF-α, IL-1β, INF-γ, and IL-6, in *V. anguillarum*-infected MO/MΦ, whereas anti-PaCCL2L decreased their expression. Our result is consistent with previous studies on mammalian CCL2, suggesting that PaCCL2L could regulate the functions of ayu MO/MΦ similar to its mammalian homologs.

In summary, we characterized a novel CCL2L gene from ayu. PaCCL2L expression in ayu tissues and MO/MΦ was induced by *V. anguillarum* infection. PaCCL2L treatment increased the survival and decreased the bacterial burden of *V. anguillarum*-infected fish. PaCCL2L mediated the migration of neutrophils, resting and M1-type MO/MΦ, and activated the MO/MΦ innate response against *V. anguillarum* infection *in vitro*. Our study investigated the primary role of PaCCL2L in ayu immune responses, but further studies on the detailed regulating mechanism are required.

Acknowledgements

The project was supported by the Program for the National Natural Science Foundation of China (31772876), the Zhejiang Provincial Natural Science Foundation of China (LZ18C190001; LY17C190003), the Scientific Innovation Team Project of Ningbo (2015C110018), and the K.C. Wong Magna Fund in Ningbo University.

Appendix A. Supplementary data

Supplementary data to this article can be found online at https://doi.org/10.1016/j.fsi.2019.02.019.

References

[1] J.W. Griffith, C.L. Sokol, A.D. Luster, Chemokines and chemokine receptors: positioning cells for host defense and immunity, Annu. Rev. Immunol. 32 (2014) 659–702.
[2] J. Choi, C. Selmi, P. Leung, T.P. Kenny, T. Roskams, M.E. Gershwin, Chemokine and chemokine receptors in autoimmunity: the case of primary biliary cholangitis, Expert Rev. Clin. Immunol. 12 (2016) 661–672.
[3] R.A. Rahimi, A.D. Luster, Chemokines: critical regulators of memory T cell development, maintenance, and function, Adv. Immunol. 138 (2018) 71–98.
[4] K. Bacon, M. Baggiolini, H. Broxmeyer, R. Horuk, I. Lindley, A. Mantovani, et al., Chemokine/chemokine receptor nomenclature, J. Interferon Cytokine Res. 22 (2002) 1067–1068.
[5] E. Peatman, Z. Liu, Evolution of CC chemokines in teleost fish: a case study in gene duplication and implications for immune diversity, Immunogenetics 59 (8) (2007) 613–623.
[6] H. Nomiyama, K. Hieshima, N. Osada, Y. Kato-Unoki, K. Otsuka-Ono, S. Takegawa, T. Izawa, A. Yoshizawa, Y. Kikuchi, S. Tanase, R. Miura, J. Kusuda, M. Nakao, O. Yoshie, Extensive expansion and diversification of the chemokine gene family in zebrafish: identification of a novel chemokine subfamily CX, BMC Genomics 9 (1) (2008) 222.
[7] Q. Fu, Y. Yang, C. Li, Q. Zeng, T. Zhou, N. Li, Y. Liu, Y. Li, X. Wang, S. Liu, D. Li, Z. Liu, The chemokinome superfamily: II. The 64 CC chemokines in channel catfish and their involvement in disease and hypoxia responses, Dev. Comp. Immunol. 73 (2017) 97–108.
[8] M.H. Lehmann, W. Kastenmuller, J.D. Kandemir, F. Brandt, Y. Suezer, G. Sutter, Modified vaccinia virus ankara triggers chemotaxis of monocytes and early respiratory immigration of leukocytes by induction of CCL2 expression, J. Virol. 83 (6) (2009) 2540–2552.
[9] H. Haller, A. Bertram, F. Nadrowitz, J. Menne, Monocyte chemoattractant protein-1 and the kidney, Curr. Opin. Nephrol. Hypertens. 25 (1) (2016) 42–49.
[10] C. Winter, K. Taut, M. Srivastava, F. Länger, M. Mack, D.E. Briles, J.C. Paton, R. Maus, T. Welte, M.D. Gunn, U.A. Maus, Lung-specific overexpression of CC chemokine ligand (CCL) 2 enhances the host defense to *Streptococcus pneumoniae* infection in mice: role of the CCL2-CCR2 axis, J. Immunol. 178 (9) (2007) 5828–5838.
[11] C. Winter, W. Herbold, R. Maus, F. Länger, D.E. Briles, J.C. Paton, T. Welte, U.A. Maus, Important role for CC chemokine ligand 2-dependent lung mononuclear phagocyte recruitment to inhibit sepsis in mice infected with *Streptococcus pneumoniae*, J. Immunol. 182 (8) (2009) 4931–4937.
[12] R.N. Gomes, M.G.A. Teixeira-Cunha, R.T. Figueiredo, P.E. Almeida, S.C. Alves, P.T. Bozza, et al., Bacterial clearance in septic mice is modulated by MCP-1/CCL2 and nitric oxide, Shock 39 (2013) 63–69.
[13] C. Li, J. Chen, Y. Shi, M. Li, Characterization of *Listonella anguillarum* as the aetiological agent of vibriosis occurred in cultured ayu (*Plecoglossus altivelis*) in Ninghai country, China, Acta Microbiol. Sin. 49 (2009) 931–937.
[14] E.M. Borroni, B. Savino, R. Bonecchi, M. Locati, Chemokines sound the alarmin: the role of atypical chemokine in inflammation and cancer, Semin. Immunol. 38 (2018) 63–71.
[15] X.J. Lu, X.Y. Hang, L. Yin, Y.Q. He, J. Chen, Y.H. Shi, C.H. Li, Sequencing of the first ayu (*Plecoglossus altivelis*) macrophage transcriptome and microarray development for investigation the effect of LECT2 on macrophages, Fish Shellfish Immunol. 34 (2) (2013) 497–504.
[16] K. Tamura, G. Stecher, D. Peterson, A. Filipski, S. Kumar, MEGA6: molecular evolutionary genetics analysis version 6.0, Mol. Biol. Evol. 30 (12) (2013) 2725–2729.
[17] H. Liu, X.J. Lu, J. Chen, Full-length and a smaller globular fragment of adiponectin have opposite roles in regulating monocyte/macrophage functions in ayu, *Plecoglossus altivelis*, Fish Shellfish Immunol. 82 (2018) 319–329.

[18] Y. Ren, S.F. Liu, L. Nie, S.Y. Cai, J. Chen, Involvement of ayu NOD2 in NF-κB and MAPK signaling pathways: insights into functional conservation of NOD2 in antibacterial innate immunity, Zool. Res. 40 (2019) 77–88.
[19] Q. Chen, X.J. Lu, M.Y. Li, J. Chen, Molecular cloning, pathologically-correlated expression and functional characterization of the colony-stimulating factor 1 receptor (CSF-1R) gene from a teleost, *Plecoglossus altivelis*, Zool. Res. 37 (2016) 96–102.
[20] Y.J. Rong, X.J. Lu, J. Chen, Molecular characterization of E-type prostanoid receptor 4 (EP4) from ayu (*Plecoglossus altivelis*) and its functional analysis in the monocytes/macrophages, PLoS One 11 (2016) e0147884.
[21] F. Guan, X.J. Lu, C.H. Li, J. Chen, Molecular characterization of mudskipper (*Boleophthalmus pectinirostris*) hypoxia-inducible factor-1α (HIF-1α) and analysis of its function in monocytes/macrophages, PLoS One 12 (2017) e0177960.
[22] J. Yu, J. Chen, Y. Li, W. Gou, W. Ji, H. Xu, Detection of *Vibrio anguillarum* from *Lateolabrax japonicus* by using polymerase chain reaction (PCR), J. Oceanogr. Huanghai Bohai Seas 20 (2002) 60–64.
[23] L. Zhang, L. Nie, S.Y. Cai, J. Chen, J. Chen, Role of a macrophage receptor with collagenous structure (MARCO) in regulating monocyte/macrophage functions in ayu, *Plecoglossus altivelis*, Fish Shellfish Immunol. 74 (2018) 141–151.
[24] F. Chen, X.J. Lu, L. Nie, Y.J. Ning, J. Chen, Molecular characterization of a CC motif chemokine 19-like gene in ayu (*Plecoglossus altivelis*) and its role in leukocyte trafficking, Fish Shellfish Immunol. 72 (2018) 301–308.
[25] J. Chen, Q. Chen, X.J. Lu, J. Chen, The protection effect of LEAP-2 on the mudskipper (*Boleophthalmus pectinirostris*) against *Edwardsiella tarda* infection is associated with its immunomodulatory activity on monocytes/macrophages, Fish Shellfish Immunol. 59 (2016) 66–76.
[26] G.T. Haugland, A. Rønneseth, H.I. Wergeland, Flow cytometry analyses of phagocytic and respiratory burst activities and cytochemical characterization of leucocytes isolated from wrasse (*Labrus bergylta* A.), Fish Shellfish Immunol. 39 (1) (2014) 51–60.
[27] B. Lu, B.J. Rutledge, L. Gu, J. Fiorillo, N.W. Lukacs, S.L. Kunkel, R. North, C. Gerard, B.J. Rollins, Abnormalities in monocyte recruitment and cytokine expression in monocyte chemoattractant protein 1-deficient mice, J. Exp. Med. 187 (4) (1998) 601–608.
[28] D.A. Zisman, S.L. Kunkel, R.M. Strieter, W.C. Tsai, K. Bucknell, J. Wilkowski, T.J. Standiford, MCP-1 protects mice in lethal endotoxemia, J. Clin. Invest. 99 (12) (1997) 2832–2836.
[29] H. Oshima, K. Hioki, B.K. Popivanova, K. Oguma, N. Van Rooijen, T.O. Ishikawa, M. Oshima, Prostaglandin E_2 signaling and bacterial infection recruit tumor-promoting macrophages to mouse gastric tumors, Gastroenterology 140 (2) (2011) 596–607.
[30] Y. Nakano, T. Kasahara, N. Mukaida, Y.C. Ko, M. Nakano, K. Matsushima, Protection against lethal bacterial infection in mice by monocyte-chemotactic and -activating factor, Infect. Immun. 62 (1994) 377–383.
[31] G.B. Huffnagle, R.M. Strieter, T.J. Standiford, R.A. Mcdonald, M.D. Burdick, S.L. Kunkel, et al., The role of monocyte chemotactic protein-1 (MCP-1) in the recruitment of monocytes and CD4+ T cells during a pulmonary *Cryptococcus neoformans* infection, J. Immunol. 155 (1995) 4790–4797.
[32] A. Matsukawa, C.M. Hogaboam, N.W. Lukacs, P.M. Lincoln, R.M. Strieter, S.L. Kunkel, Endogenous monocyte chemoattractant protein-1 (MCP-1) protects mice in a model of acute septic peritonitis: cross-talk between MCP-1 and leukotriene B_4, J. Immunol. 163 (1999) 6148–6154.
[33] B.J. Rollins, A. Walz, M. Baggiolini, Recombinant human MCP-1/JE induces chemotaxis, calcium flux, and the respiratory burst in human monocytes, Blood 78 (1991) 1112–1116.
[34] G. Balamayooran, S. Batra, T. Balamayooran, S. Cai, S. Jeyaseelan, Monocyte chemoattractant protein 1 regulates pulmonary host defense via neutrophil recruitment during *Escherichia coli* infection, Infect. Immun. 79 (7) (2011) 2567–2577.
[35] S. Yamashiro, M. Takeya, T. Nishi, J.I. Kuratsu, T. Yoshimura, Y. Ushio, et al., Tumor-derived monocyte chemoattractant protein-1 induces intratumoral infiltration of monocyte-derived macrophage subpopulation in transplanted rat tumors, Am. J. Pathol. 145 (1994) 856–867.
[36] T. Tsuchiyama, Y. Nakamoto, Y. Sakai, N. Mukaida, S. Kaneko, Optimal amount of monocyte chemoattractant protein–1 enhances antitumor effects of suicide gene therapy against hepatocellular carcinoma by M1 macrophage activation, Cancer Sci. 99 (10) (2008) 2075–2082.
[37] S. Iida, T. Kohro, T. Kodama, S. Nagata, R. Fukunaga, Identification of CCR2, flotillin, and gp49B genes as new G-CSF targets during neutrophilic differentiation, J. Leukoc. Biol. 78 (2) (2005) 481–490.
[38] G. Weiss, U.E. Schaible, Macrophage defense mechanisms against intracellular bacteria, Immunol. Rev. 264 (1) (2015) 182–203.
[39] Q. Wang, J. Ren, S. Morgan, Z. Liu, C. Dou, B. Liu, Monocyte chemoattractant protein-1 (MCP-1) regulates macrophage cytotoxicity in abdominal aortic aneurysm, PLoS One 9 (2014) e92053.